Entropy **2003**, *5*, 366–376

Entropy
ISSN 1099-4300
www.mdpi.org/entropy/

Vibrational Effect on Entropy Generation in a Square Porous Cavity

Shohel Mahmud[1] and Roydon Andrew Fraser[2]

[1]Department of Mechanical Engineering, University of Waterloo, Waterloo, Ontario Canada. Tel. +1 519 888 4567; Fax +1 519 888 6197; Email: smahmud@uwaterloo.ca
[2]Email: rafraser@uwaterloo.ca

Received: 7 December 2002 / Accepted: 10 June 2003 / Published: 31 December 2003

Abstract: We investigate the nature of entropy generation for natural convection in a two-dimensional square section enclosure vibrating sinusoidally perpendicular to the applied temperature gradient in a zero-gravity field. The enclosure is assumed to fill with porous media. The Darcy momentum equation is used to model the porous media. The full governing differential equations are simplified with the Boussinesq approximation and solved by a finite volume method. Whereas the Prandtl number Pr is fixed to 1.0. Results are presented in terms of average Nusselt number (Nu_{av}), entropy generation number (Ns_{av}), Bejan number (Be_{av}), and kinetic energy (KE_{av}).

Keywords: vibrational convection, entropy generation, porous media, Bejan number, square cavity.

Introduction

Free convection heat transfer inside a square cavity (porous or non-porous) is a well-established problem. During last two decades, a vast number of articles have been published in this field. For a comprehensive reference see Bejan [1]. Free convection inside a square cavity with gravity oscillation is a special class of above-mentioned problem. In low gravity or microgravity environments, we can expect that reduction or elimination of natural convection may enhance the properties and performance

of materials such as crystals (Hirata *et al*. [2]). However, aboard orbiting spacecrafts all objects experience low-amplitude broadband perturbed accelerations, or g-jitter, caused by crew activities, orbiter maneuvers, equipment vibrations, solar drag, and other sources. Therefore, there is growing interest in understanding the effects of these perturbations on the system behavior. The reference articles by Hirata *et al*. [2], Biringen and Danabasoglu [3], Gershuni and Zhukhovitskiy [4], Goldhirsch *et al*. [5], Kamotani *et al*. [6], and Kondos and Subramanian [7] will give a clear idea of flow and thermal fields behavior inside enclosures under gravity oscillation. Until now, there have been no reported research activities, which systematically elucidate the effects of gravity oscillation on the entropy generation rate inside enclosures under buoyantly driven flows in a microgravity environment. Most of the published analyses have been restricted, from a thermodynamic point of view, to only First-Law (of thermodynamics) analyses. The contemporary trend in the field of heat transfer and thermal design is to perform a Second-Law (of thermodynamics) analysis, and to perform its design-related analysis of entropy generation minimization (Bejan [8]). Entropy generation minimization is the method of modeling and optimization of real devices that owe their thermodynamic imperfection to heat transfer, mass transfer, and fluid flow irreversibilities. It is also known as *thermodynamic optimization* in engineering, where it was first developed, or more recently as *finite space-time thermodynamics* in the physics literature (Bejan [9]). Entropy generation minimization combines into simple models the most basic concepts of heat transfer, fluid mechanics, and thermodynamics. These simple models are used in the optimization of real (irreversible) devices and processes, subject to finite-size and finite-time constraints that are in fact responsible for the irreversible operation of the device. So, for proper use of this method, an analyst must know the behavior of system's irreversibilities in terms of entropy generation and the variation of irreversibilities with system parameters (flow parameters, transport properties, geometry etc.).

Therefore, in the present work, we study the entropy generation characteristics inside a porous cavity by solving numerically the fully nonlinear time-dependent momentum and energy equations in a two-dimensional Cartesian frame. More specifically, the cavity has perfectly isothermal and differentially heated sidewalls and adiabatic top and bottom walls. The gravity oscillation is assumed to follow a perfect sine wave. Results are presented for three different Rayleigh numbers (Ra=50,100, and 500) and two different frequencies of oscillation.

Equations and Numerical Methods

Figure 1 shows the domain to be analyzed and the adopted coordinate system. All asterisked quantities in this paper are in dimensional form. Fluid in a two-dimensional cavity with a square cross-section is subject to sinusoidal acceleration parallel to the vertical axis in a zero-gravity field. Upper and lower walls, parallel to the horizontal axis, are adiabatic. Left and right walls are isothermal. It is assumed that the cavity is completely filled with the fluid. Uneven density of fluid originating from the temperature difference of the walls produces buoyancy and drives convection due to fluctuating

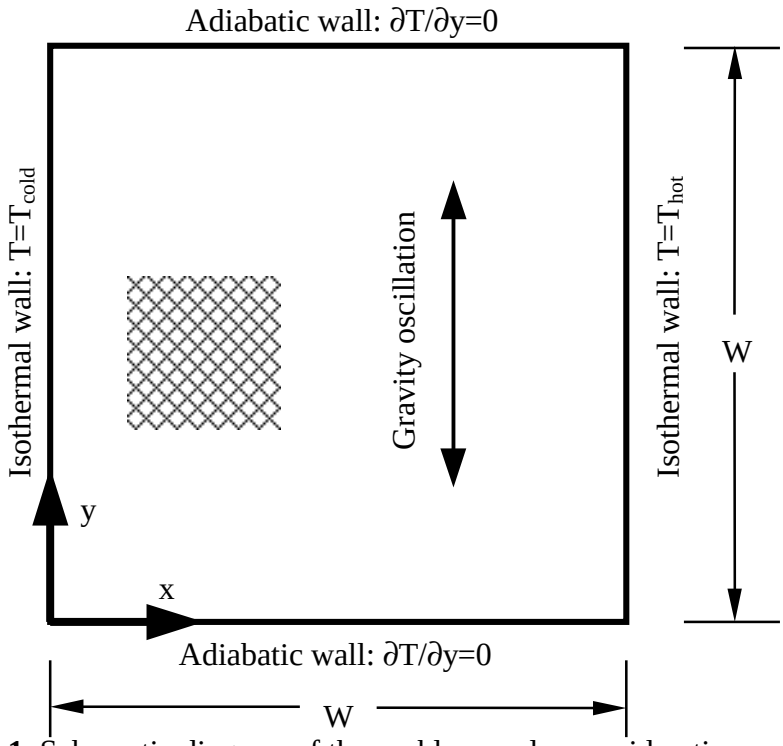

Figure 1. Schematic diagram of the problem under consideration

acceleration. The saturated porous medium is assumed to be isotropic in thermal conductivity and follows the Darcy model (Bejan [1]). Finally, the set of non-dimensional governing equations in terms of the stream function ψ and temperature Θ are

$$\frac{\partial^2\psi}{\partial x^2}+\frac{\partial^2\psi}{\partial y^2}=Ra\frac{\partial\Theta}{\partial x}\sin(\omega\tau), \tag{1}$$

$$\frac{\partial\Theta}{\partial\tau}+\frac{\partial\psi}{\partial y}\frac{\partial\Theta}{\partial x}-\frac{\partial\psi}{\partial x}\frac{\partial\Theta}{\partial y}=\frac{\partial^2\Theta}{\partial x^2}+\frac{\partial^2\Theta}{\partial y^2}, \tag{2}$$

$$\begin{aligned}
&x=\frac{x^*}{W},\ y=\frac{y^*}{W},\ \psi=\frac{\psi^*}{\alpha},\ \Theta=\frac{T-T_0}{\Delta T},\ \Delta T=T_{\text{hot}}-T_{\text{cold}},\ T_0=\frac{T_{\text{hot}}+T_{\text{cold}}}{2}\\
&\tau=t\left(\frac{\alpha}{W^2\sigma}\right),\ Ra=\frac{gK\beta\Delta TW}{\alpha\nu},\omega=\frac{\omega^*\sigma W^2}{\alpha},u=\frac{\partial\psi}{\partial y},v=-\frac{\partial\psi}{\partial x}\\
&\sigma=\frac{\phi\rho C_p+(1-\phi)\rho_s C_s}{\rho C_p},
\end{aligned} \tag{3}$$

subjected to the following boundary conditions

$$\begin{aligned}
&\tau > 0,\ y = 0,\ 0 \ge x \ge 1 : \psi = 0 \text{ and } \partial\Theta/\partial y = 0 \\
&\tau > 0,\ y = 1,\ 0 \ge x \ge 1 : \psi = 0 \text{ and } \partial\Theta/\partial y = 0 \\
&\tau > 0,\ x = 0,\ 0 \ge y \ge 1 : \psi = 0 \text{ and } \Theta = -0.5 \\
&\tau > 0,\ x = 1,\ 0 \ge y \ge 1 : \psi = 0 \text{ and } \Theta = 0.5.
\end{aligned} \tag{4}$$

The meaning of different parameter of Eqs. (1)–(4) are given in nomenclature section. Equations (1) and (2) along with the boundary conditions given in Eq. (4) are solved using control volume based Finite-Volume method. A non-staggered and non-uniform grid system is used with a higher mesh density near the walls. TDMA solver solves discretized and linearized equation systems. For unsteady terms, Crank-Nicolson method is applied. The whole computational domain is subdivided by an unequally spaced rectangular mesh with a size of 128×128. The time increment ($\Delta\tau$) was 10^{-4} in most cases; but sometimes, especially at high *Ra* smaller values were chosen in order to confirm the accuracy of the results.

Entropy Generation

The dimensionless form of entropy generation rate (S'''_{gen}) is termed as entropy generation number (Bejan [8]). Entropy generation number (*Ns*) is the ratio between entropy generation rate (*Ns*) and a characteristics transfer rate (S'''_0). The characteristics transfer rate for the present problem can be estimated from the following equation:

$$S'''_0 = \frac{k(\Delta T)^2}{W^2 T_0^2}. \tag{5}$$

For the porous media, which follows the Darcy model, the local rate of entropy generation (S'''_{gen}) can be calculated from the following equation:

$$S'''_{\text{gen}} = \frac{k}{T_0^2}\left(\vec{\nabla}\mathbf{T}\right)^2 + \frac{\mu}{KT_0}\left(\vec{\mathbf{V}}\right)^2. \tag{6}$$

The detailed derivation of the above equation is available in Bejan [1]. The dimensionless form of Eq. (6) gives the expression of entropy generation number as

$$N_S = \frac{S'''_{gen}}{S'''_0} = \left[\left(\frac{\partial\Theta}{\partial x}\right)^2 + \left(\frac{\partial\Theta}{\partial y}\right)^2\right] + \frac{Ec_m \times \Pr}{\Omega}\left[\left(\frac{\partial\psi}{\partial x}\right)^2 + \left(\frac{\partial\psi}{\partial y}\right)^2\right], \tag{7}$$

which consists of two parts. The first part (first square bracketed term at the right-hand side of Eq. (7)) is the irreversibility due to finite temperature gradient and generally termed as heat transfer irreversibility (HTI). The second part is the contribution of fluid friction irreversibility (FFI) to entropy generation, which can be calculated from the second square bracketed term. The overall entropy generation, for a particular problem, is an internal competition between HTI and FFI. Usually, free convection problems, at low and moderate Rayleigh numbers, are dominated by the heat transfer irreversibility. Entropy generation number (N_S) is good for generating entropy generation profiles or

maps but fails to give any idea whether fluid friction or heat transfer dominates. Two alternate parameters, irreversibility distribution ratio (Φ) and Bejan number (*Be*), are achieving an increasing popularity among the Second-Law analysts. Bejan number (*Be*), which is the ratio of HTI to the total entropy generation, can be mathematically expressed as

$$Be = \frac{\mathrm{HTI}}{\mathrm{HTI} + \mathrm{FFI}}. \tag{8}$$

Bejan number ranges from 0 to 1. Accordingly, *Be*=1 is the limit at which the heat transfer irreversibility dominates, *Be*=0 is the opposite limit at which the irreversibility is dominated by fluid friction effects, and *Be*=1/2 is the case in which the heat transfer and fluid friction entropy generation rates are equal.

Table 1: Comparison of average Nusselt number with some previous numerical results

	Nu_{av}		
	Ra=10	Ra=100	Ra=1000
Baytas and Pop [10]	1.079	3.16	14.06
Walker and Homsy [11]	--------	3.10	12.96
Gross *et al*. [12]	--------	3.14	13.45
Manole and Lage [13]	--------	3.12	13.64
Moya *et al*. [14]	1.065	2.80	-------
Present prediction	1.079	3.14	13.82

Results and discussion

For the benchmarking purpose, a differentially heated square porous cavity under constant gravitational force is considered. Average Nusselt number is calculated for three different Rayleigh numbers (*Ra*=10, 100, and 1000) and compared with the available published works [10–14]. This comparison is shown in Table 1. It is seen from Table 1 that the agreement between the present and the previous results is very good. Therefore, we are confidant that the numerical method used and the results presented in this paper are very accurate.

At first we start with the heat transfer characteristics inside the cavity. Rate of heat transfer is measured in terms of the dimensionless Nusselt number. Once the gravity vibration is introduced (at time $\tau = \tau_0$), it takes some time to set the convective motion inside the cavity. Determination of this time is beyond the scope of this paper. For the details about the setup time and instability, see reference by Gershuni and Lyubimov [15]. At a particular time ($=\tau_0+\mathrm{m}.\Delta\tau$, m=0,1,2…), normal component of the temperature gradient ($\partial\Theta/\partial n|_w$) near each wall is measured which is a function of distance and time. An integration is then carried out using the following equation

$$Nu_{av} = Nu_{av}(\tau) = \frac{1}{2}\oint_{\Gamma}\left|\frac{\partial\Theta}{\partial n}\right| ds \tag{9}$$

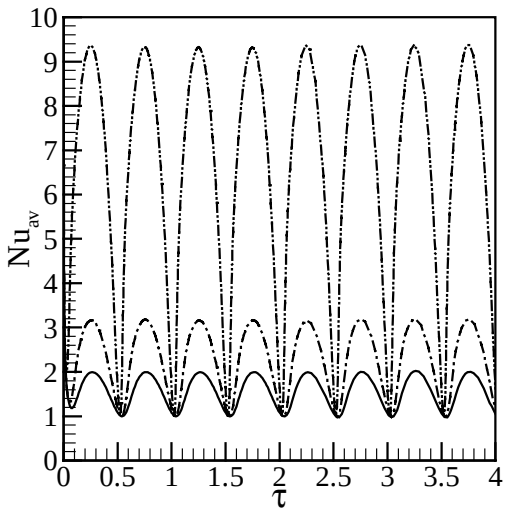

Figure 2. Average Nusselt number (Nu_{av}) as a function of dimensionless time (τ) at $\omega=2\pi$ and Ra=50 (solid line), 100 (dash-dot line), and 500 (dash-dot-dot line

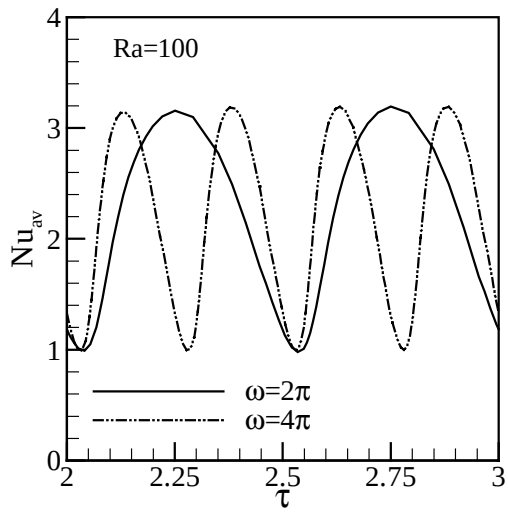

Figure 3. Average Nusselt number (Nu_{av}) as a function of dimensionless time (τ) at $\omega=2\pi$ and 4π and Ra=100

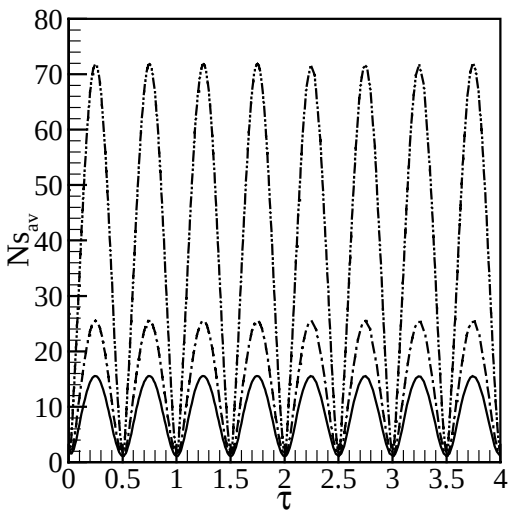

Figure 4. Average entropy generation number (Ns_{av}) as a function of dimensionless time (τ) at $\omega=2\pi$ and Ra=50 (solid line), 100 (dash-dot line), and 500 (dash-dot-dot line).

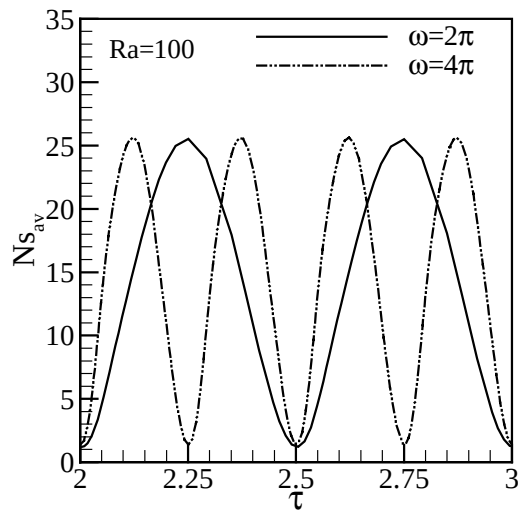

Figure 5. Average entropy generation number (Ns_{av}) as a function of dimensionless time (τ) at $\omega=2\pi$ and 4π and Ra=100

along the whole boundary of the cavity (see Gershuni and Lyubimov [15]) to get spatially averaged Nusselt numbers (Nu_{av}) as a function of dimensionless time. For a limited time interval, $0 > \tau \geq 4$,

variation of Nusselt number (Nu_{av}) is reported as a function of time (τ) in Figure 2 for three different Rayleigh numbers. In real simulation, the total time is much higher than this time interval. It is evident from Figure 2 that an induced gravity oscillation introduces a true periodic behavior to the average heat transfer rate inside the cavity. As we used the absolute value of the normal component of the temperature gradient (see Eq. (9)) during the calculation of average Nusselt number, the fluctuation of Nu_{av} appears at the positive half of the Nu_{av}–τ plot. The periodic response of Nu_{av} is synchronized with the forced acceleration, namely, having the same period as the forced acceleration. At the upper extreme of the oscillation ($\omega\tau$ = (2m-1)π/2, m=1,2,3…) the magnitude of Nu_{av} approaches the corresponding value of Nu_{av} at steady state and constant gravity. At the lower extreme of the oscillation ($\omega\tau = m\pi$, m=1,2,3…) gravity force disappears. Heat transfer inside the cavity occurs in conduction mode. For all Rayleigh numbers, Nu_{av} is same and equal to 1. Effect of ω on Nu_{av} is shown in Figure 3 for Ra=100. Synchronous relation between gravity oscillation and the Nu_{av}–τ profile is observed from the figure. Two extreme Nusselt numbers remain same for both values of ω.

The local entropy generation rate (Ns) and Bejan number (Be) are calculated using Eqs. (7) and (8), respectively. Both Ns and Be are function of spatial coordinates and time. The volume averaged value of entropy generation number (Ns_{av}) and Bejan number (Be_{av}) can be calculated from the following equations:

$$Ns_{av} = Ns_{av}(\tau) = \frac{1}{\forall}\int_{\forall} Ns(x, y, \tau)\, d\forall, \tag{10}$$

$$Be_{av} = Be_{av}(\tau) = \frac{1}{\forall}\int_{\forall} Be(x, y, \tau)\, d\forall, \tag{11}$$

where $\forall$ represents the volume of the cavity. Average entropy generation number (Ns_{av}) is plotted as a function of dimensionless time in Figure 4 for three different values of Rayleigh number. The Ns_{av}–τ behavior is similar to the Nu_{av}–τ behavior as already described. The periodic response of the average entropy generation number is synchronized with the gravity oscillation. At a particular time (τ), irreversibility is higher at high Rayleigh number, but the maximum value of Ns_{av} obtained for any Rayleigh number when gravity oscillation reaches its upper extreme ($\omega\tau$ = (2m-1)π/2, m=1,2,3…). In the absence of the gravity ($\omega\tau = m\pi$, m=1,2,3…) irreversibilities at all Rayleigh numbers are same and show their minimum. Effect of ω on Ns_{av} is shown in Figure 5 for Ra=100. Synchronous relation between gravity oscillation and the Ns_{av}–τ profile is observed from the figure. Two extreme entropy generation numbers remain same for both values of ω. However, average Bejan number (Be_{av}) distribution remains synchronized with gravity oscillation, but it shows a complicated behavior with Rayleigh number variation in a particular time period (for example τ = 2 to 3). Figures (6)–(8) show the distribution of average Bejan number as a function of dimensionless time at Ra=50, 100, and 500, respectively. At the lower extreme of the gravity oscillation, due to the absence of the gravitational force, convective motion inside the cavity is absent. This causes the maximum dominance of heat transfer irreversibility (HTI). Average Bejan number reaches its maximum value (=1) at this extreme of

oscillation. For all Rayleigh numbers, Be_{av} shows its minimum at the upper extreme of the oscillation where convection motion is well set and fluid friction irreversibility has a reasonable domination over

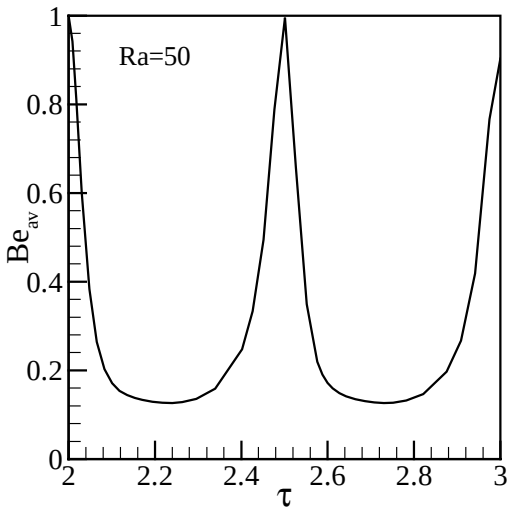

Figure 6. Average Bejan number (Be_{av}) as a function of dimensionless time (τ) at Ra=50.

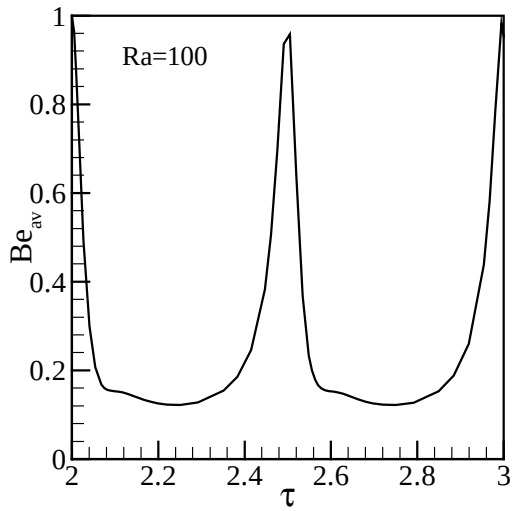

Figure 7. Average Bejan number (Be_{av}) as a function of dimensionless time (τ) at Ra=100.

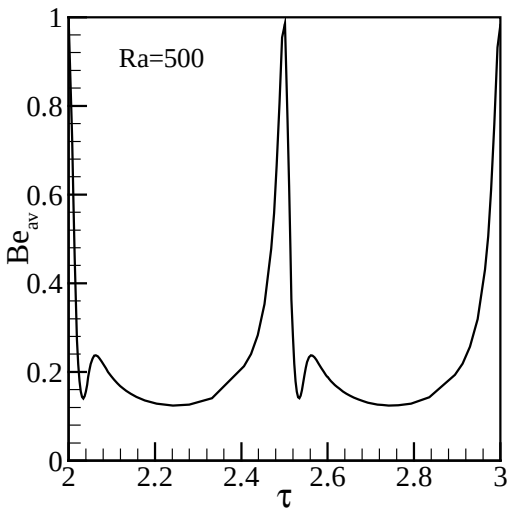

Figure 8. Average Bejan number (Be_{av}) as a function of dimensionless time (τ) at Ra=500

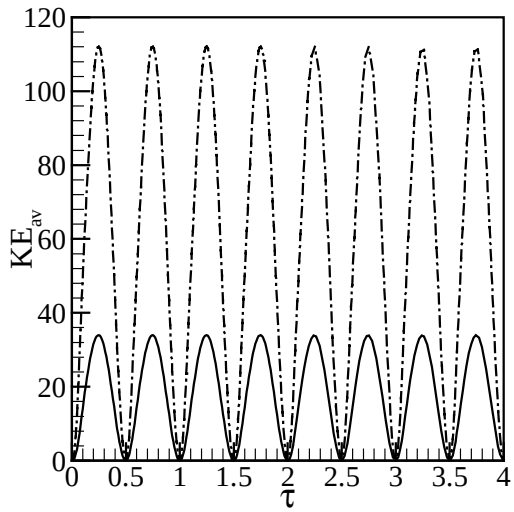

Figure 9. Average kinetic energy (KE_{av}) as a function of.

heat transfer irreversibility. At *Ra*=500, boundary layer type flow is commonly observed at steady state and constant gravity situation (see Baytas [16], Baytas and Pop [10]). However, for the situation where the flow field is under the effect of gravity oscillation, no immediate formation of hydrodynamic and thermal boundary layers. At the beginning of the oscillation (say at $\tau = 2$ as shown in Figure 8) no gravity force exists as well as no fluid friction irreversibility (FFI). Conduction dominated heat transfer

causes only small contributions to the heat transfer irreversibility (HTI). With the absence of FFI, 100% contribution of total irreversibility comes from the HTI and the corresponding Be_{av} is equal to 1 (see Figure 8). A nonzero gravity component appears just after the beginning time (τ = 2), which immediately set the convective motion inside the cavity. A positive contribution to the overall entropy generation rate now comes from the FFI. Average Bejan number then rapidly drop to a small value within a small time. Because within this short time gap, hydrodynamic boundary layer forms and thermal boundary layer is still in its developing stage. After formation, the additional modification of hydrodynamic boundary layer with the advancing time is slow and by this time thermal boundary layer is getting its final shape with increasing temperature gradient as well as HTI. This is the main reason for a small jump in the Be_{av}–τ profile between τ = 2.04 to τ = 2.12. Then Be_{av} slowly drops to its minimum value up to the upper extreme of the oscillation. Finally, the spatially averaged kinetic energy (see Hirata *et al*. [2]) is calculated according to the following equation:

$$KE_{av} = KE_{av}(\tau) = \frac{1}{2A}\int\int\left(u^2 + v^2\right)dx\,dy, \tag{12}$$

where A is the cross-sectional area of the cavity. Average kinetic energy (KE_{av}) serves as a *global indicator* of responses (see Hirata *et al*. (2001) [2]). Distribution of KE_{av} as a function of τ is shown in Figure 9 for two Rayleigh numbers (Ra=50 and 100). The synchronous behavior of the KE_{av}–τ profile with gravity oscillation is similar to the Nu_{av}–τ or Ns_{av}–τ profile as described earlier.

Conclusions

A numerical solution of the governing momentum and energy equation for a porous square cavity is presented which shows the responses of heat transfer, heat transfer irreversibility, and total irreversibility under gravity oscillation condition. Average Nusselt number (Nu_{av}), Bejan number (Be_{av}), and entropy generation number (Ns_{av}) are used for the corresponding measuring tool for above parameters. Gravity oscillation introduces a true periodic behavior to the Nusselt number, Bejan number, and entropy generation rate. The periodic response of these three parameters is synchronized with the forced acceleration, namely, having the same period as the forced acceleration. At the lower extreme of the gravity oscillation Nu_{av} and Ns_{av} is minimum and Be_{av} is maximum. This scenario reverses at the upper extreme of the gravity oscillation.

Nomenclature

A	Area of the cavity, m^2.
Be	Bejan number, (see Eq. (8)).
C_p	Specific heat of the fluid, $J.kg^{-1}.^0C^{-1}$.
C_s	Specific heat of the solid matrix, $J.kg^{-1}.^0C^{-1}$.
Ec_m	Modified Eckert number = $u_0^2 W^2 / \left(C_p.K.\Delta T\right)$.
K	Permeability of the porous media, m^2.

KE	Kinetic energy, J.
Ns	Entropy generation number, (see Eq. (7)).
Nu	Nusselt number, (see Eq. (9)).
Pr	Prandtl number = ν/α.
Ra	Rayleigh number, (see Eq. (3)).
S'''_{gen}	Entropy generation rate, W.m^{-3}.K^{-1}.
S'''_0	Characteristics entropy transfer rate, (see Eq. (5)).
T	Temperature of the fluid, ^{0}C.
T_0	Reference temperature, ^{0}C.
t	Time, sec.
u^*	x-component of the velocity, m.sec^{-1}.
v^*	y-component of the velocity, m.sec^{-1}.
u	x-component of the dimensionless velocity = u^*/u_0.
v	y-component of the dimensionless velocity = v^*/u_0.
u_0	Reference velocity = α/W.
W	Width and height of the cavity, m.
x^*	Horizontal distance, m.
y^*	Vertical distance, m.
x	Dimensionless horizontal distance =x^*/W.
y	Dimensionless vertical distance =y^*/W.
	Greek symbols
α	Thermal diffusivity of the fluid, m^2.sec^{-1}.
β	Thermal expansion coefficient of the fluid, ^{0}C^{-1}.
ψ^*	Streamfunction, m^2.sec^{-1}.
ψ	Dimensionless streamfunction = ψ^*/α.
Θ	Dimensionless temperature = $(T-T_0)/\Delta T$.
ω^*	Angular frequency, Hz.
ω	Dimensionless angular frequency, (see Eq. (3)).
ρ	Density of the fluid, kg.m^{-3}
ρ_s	Density of the solid matrix, kg.m^{-3}
τ	Dimensionless time = $t.\alpha/(W^2.\sigma)$.
σ	Empirical constant (see Eq. (3))
ν	Kinematic viscosity of the fluid, m^2.sec^{-1}.
$\forall$	Volume of the cavity, m^3.
ϕ	Porosity of the porous media.

References

[1] A. Bejan, *Convection Heat Transfer* (John Wiley & Sons, New York, 1984).

[2] Hirata, K., Sasaki, T., Tanigawa, H. Vibrational effects on convection in a square cavity at zero gravity. J. Fluid Mechanics. 2001, 445, 327–344.

[3] Biringen, S., Danabasoglu, G. Computation of convective flow with gravity modulation in rectangular cavities. J. Thermophys. 1990, 4, 357–365.

[4] Gershuni, G.Z., Zhukhovitskiy, Y.M. Vibration-induced thermal convection in weightlessness. Fluid Mech.–Sov. Res. 1986, 15, 63–84.

[5] Goldhirsch, I., Pelz, R.B., Orszag, S.A. Numerical simulation of thermal convection in a two-dimensional finite box. J. Fluid Mech. 1989,199, 1–28.

[6] Kamotani, Y., Prasad, A., Ostrach, S. Thermal convection in an enclosure due to vibrations aboard spacecraft. AIAA J. 1981, 19, 511–516.

[7] Kondos, P.A., Subramanian, R.S. Buoyant flow in a two-dimensional cavity due to a sinusoidal gravitational field. Microgravity Sci. Technol. 1996, 9, 143–151.

[8] A. Bejan, *Entropy Generation Minimization* (CRC Press, New York, 1996).

[9] Bejan, A. Fundamental of exergy analysis, entropy generation minimization, and the generation of flow architecture. Int. J. Energy Research. 2002, 26, 545–565.

[10] Baytas, A.C., Pop, I. Free convection in oblique enclosures filled with a porous medium. Int. J. Heat Mass Transfer. 1999, 42, 1047–1057.

[11] Walker, K.L., Homsy, G.M. Convection in a porous cavity. J. Fluid Mechanics. 1978, 87, 449–474.

[12] Gross, R.J., Bear, M.R., Hickox, C.E. The application of flux-corrected transport (FCT) to high Rayleigh number natural convection in porous medium, in: Proc. 8th International Heat Transfer Conference, San Francisco, CA, 1986.

[13] Manole, D.M., Lage, J.L. Numerical benchmark results for natural convection in a porous medium cavity, HTD-Vol. 216, Heat and Mass Transfer in Porous Media, ASME Conference 1992, pp. 55–60.

[14] Moya, S.L., Ramos, E., Sen, M. Numerical study of natural convection in a tilted rectangular porous material. Int. J. Heat Mass Transfer, 1987, 30, 741–756.

[15] Gershuni, G.Z., Lyubimov, D.V. *Thermal Vibrational Convection* (John Wiley & Sons, New York, 1997).

[16] Baytas A.C. Entropy generation for natural convection in an inclined porous cavity, Int. J. Heat and Mass Transfer, 2000, 43, 2089–2099.